

## Effects of Oxygen Interaction with PbTe Surface and Their Influence on Thermoelectric Material Properties

I.V. Horichok<sup>1</sup>, V.V. Prokopiv<sup>1</sup>, R.I. Zapukhlyak<sup>1</sup>, O.M. Matkivskyj<sup>1</sup>,  
T.O. Semko<sup>1</sup>, I.O. Savelikhina<sup>2</sup>, T.O. Parashchuk<sup>3</sup>

<sup>1</sup> *Vasyl Stefanyk Precarpathian National University, 57, Shevchenko Str., 76018 Ivano-Frankivsk, Ukraine*

<sup>2</sup> *Ivano-Frankivsk National Medical University, 2, Halytska Str., 76018 Ivano-Frankivsk, Ukraine*

<sup>3</sup> *The Institute of Advanced Manufacturing Technology, 37, Wroclawska Str., 30-011 Krakow, Poland*

(Received 12 August 2018; revised manuscript received 24 October 2018; published online 29 October 2018)

The results of the study of thermoelectric material properties obtained by pressing the powder of lead telluride samples are presented. It is shown that an adequate model of pressed samples structure should take into account the presence of a near-surface layer, which formation is associated with the interaction of the material with atmospheric oxygen. The calculation of carrier mobility in the samples has been spent with considering the mechanisms of carrier dispersion on acoustic phonons and thermoelectronic emission.

**Keywords:** Lead Telluride, Thermoelectrical parameters, Diffusion, Surface oxidation.

DOI: [10.21272/jnep.10\(5\).05006](https://doi.org/10.21272/jnep.10(5).05006)

PACS numbers: 72.15.Jf, 61.72.uj

### 1. INTRODUCTION

The investigation of alternative energy sources, in particular thermoelectric generators (TEG), is an actual scientific task. The main advantages of devices that convert heat energy into electric are high reliability and significant period of uninterrupted operation. Despite this, the lack of TEG is a relatively low efficiency factor, which, as a rule, does not exceed 10 % in industrial samples. Lead Telluride, despite the active search for alternative materials based on less toxic components, remains one of the best semiconductor materials for the creation of TEG operating in (200-500) °C temperature range [1-3].

The efficiency of materials used in thermoelectric converters is determined by the magnitude of the thermoelectric figure of merit  $Z$ , which is directly proportional to the specific electrical conductivity, the square of the thermo-EMF coefficient, and the inversely proportional to the thermal conductivity coefficient. Due to its crystalline and energy structures, high values of  $Z$  parameter can be achieved even for the pure lead telluride [4].

A promising area is the study of thermoelectric samples obtained by powder pressing, which provides a large area of intergranular boundaries and, accordingly, low values of the thermal conductivity coefficient. One of the methods of powders pressing is the compression in the air with subsequent annealing in vacuum, argon or Hydrogen. In this case, the interaction of material surface with atmospheric oxygen is logical. According to published data [5, 6], such interaction can lead to the formation of a surface layer with properties that are different from the properties of the central part of the grains that are pressed. However, there are no clear conclusions about the structure and properties of this layer in the literature. In addition, according to [7], if the pressing occurs at high pressures that we used in this study, the oxidized surface layer can be shaken and its effect on the properties of the pressed sample will be insignificant in the whole.

That said, the aim of this work is to establish the

peculiarities of kinetic processes in the samples obtained by compression in the air and subsequent annealing, the influence of surface effects and intergranular boundaries on them.

### 2. RESEARCH METHODS

Synthesis of lead telluride was carried out in sealed quartz ampules. The phase composition and parameter of the elementary cell were determined by X-ray diffraction methods at DRON-3 and STOE STADI P. Microhardness and surface structure were investigated on a NEXUS A412 micro-volume meter and on MIII-4 interferometer. Samples for research were obtained by pressing the powder [8]. The coefficient of thermo-EMF was determined by measuring the magnitude of the thermoelectric motive force on the sample at a temperature gradient at its ends  $\approx 10$  °C. The electrical conductivity was determined by measuring the voltage difference across the sample at passage through it alternating current. The method of radial heat flux was used to determine the coefficient of thermal conductivity. Computer simulation and processing of the results of experiments were carried out using application programs MAPLE 9.5 and EXCEL.

### 3. THE RESULTS OF EXPERIMENT

Based on X-ray studies, it was found that synthesized ingots and samples made on their basis by the powder pressing method are single-phase, structural type NaCl. Parameter of element cell for bars is  $a_{\text{ingot}} = 6,4577 \pm 0,0010 \text{ \AA}$  and for a pressed and annealed sample – ( $a_{\text{sample}} = 6,4564 \pm 0,0010 \text{ \AA}$ ).

The carrier concentration, determined at the Hall effect study, is  $\approx 2 \cdot 10^{18} \text{ cm}^{-3}$  at 30 °C and  $\approx 1 \cdot 10^{18} \text{ cm}^{-3}$  at 150 °C. Relatively low concentrations of carriers indicate a minor deviation of the stoichiometry of samples in the process of performing their operations.

Typical temperature dependences of thermoelectric parameters of non-dopant lead telluride are shown in fig. 1. Properties of non-annealed samples and annealed

at  $T = 230$  °C are practically identical. At temperatures below 200 °C samples show the hole type conductivity. The coefficient of thermo-EMF at 100 °C is  $\approx 400$   $\mu\text{V}/^\circ\text{C}$ . With the temperature rising to about 200 °C the conductivity type changes to the electron and at 300 °C  $\alpha \approx 250$   $\mu\text{V}/^\circ\text{C}$ . The temperature dependence of the electrical conductivity for all samples is nonmonotonic with a minimum at a temperature corresponding to the p-n-junction.

Annealing at 500 °C leads to a significant increase of the electrical conductivity of the material, which exhibits only p-type conductivity in the studied range of temperatures.

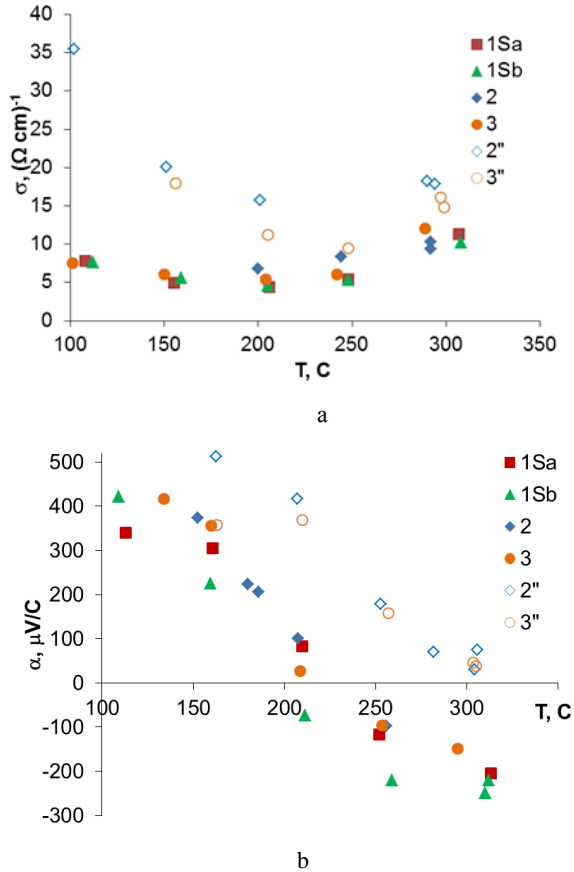


**Fig. 1** – Temperature dependence of specific conductivity  $\sigma$  (a) and coefficient of thermo-EMF  $\alpha$  (b) of the samples of PbTe (XV) obtained by pressing powder (0.05-0.5) mm under pressure of 2 GPa. The samples 1Sa, 1Sb were annealed at 230 °C, 2, 3 were not annealed, 2'', 3'' were annealed at 500 °C

#### 4. ANALYSIS OF THE RESULTS OF THE EXPERIMENT

The reason for qualitative changes in the electrical conductivity of the material after the annealing can be as a restructuring of the grain boundaries, fixed in the study of the samples surface of [8], and, also, the modification of its defective subsystem. However, according to [9, 10], the defective subsystem PbTe almost completely hardens at significantly higher temperatures than 500 °C. Thus, the reduction of the resistance between the grains from which the sample is compressed is the most likely cause by growth of the  $\sigma$  value.

If the measured dependences of the specific conduc-

tivity and the temperature represent in the coordinates  $\ln(\sigma) \cdot 1/T$ , then in the high temperature range the slope of the experimental dependences corresponds to the activation energy of 0.38 eV corresponding to the PbTe band gap. After annealing, the slope of the investigated dependence does not change, although the free parameter of the dependence  $\ln(\sigma) = -E_g/2kT + A$  increases.

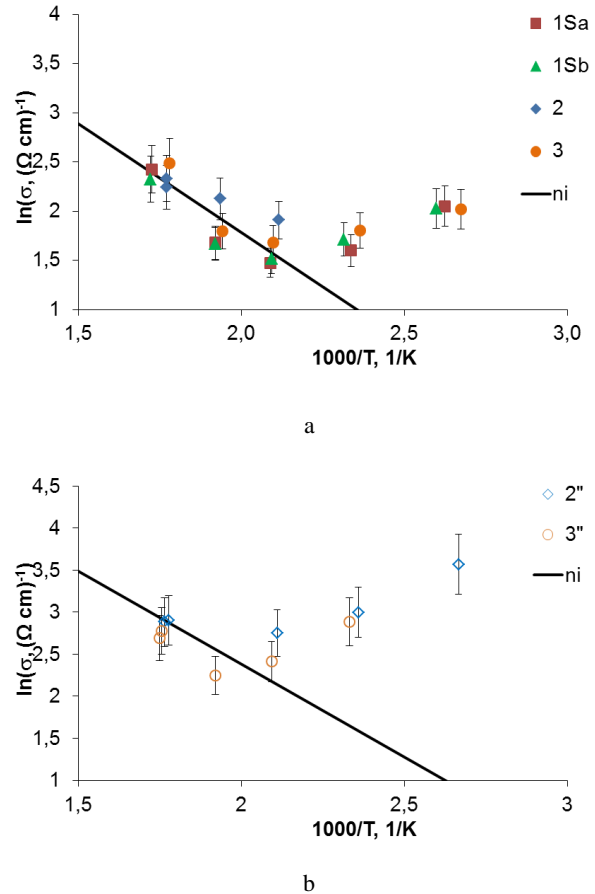


**Fig. 2** – The dependence of the logarithm of conductivity and the inverse temperature for the samples of non-doped PbTe before the annealing (a) and after annealing (b) at a temperature of 500 °C. The straight line corresponds to the dependence  $\ln(\sigma) = -0.38/2kT + A$ .

In order to explain the nature of the dependences of thermoelectric parameters at below 200 °C temperatures, and also considering the compression of samples is carried out in air, we agreed a model for the formation of a near-surface layer of  $p$ -type conductivity, due to the interaction of the grain surface with atmospheric oxygen.

The distribution of oxygen at the depth of the sample can be calculated based on diffusion equations [11]. If diffusion occurs from the surface layer, the surface oxygen concentration in which is finite and is equal to  $A$  (a limited source), then its distribution at the depth  $x$  at time  $t$  is determined according to equation:

$$N(x, t) = \frac{A}{\sqrt{\pi Dt}} \exp\left(-\frac{x^2}{4Dt}\right),$$

where  $D$  is the coefficient of oxygen diffusion. If the

concentration of atoms in some near-surface layer is a constant value of  $N_0$ , then the new (unrestricted source) suitable for the diffusion of atoms into the sample approaches, then the distribution of oxygen in depth is determined according to equation:

$$N(x,t) = N_0 \operatorname{erfc} \left( \frac{x}{\sqrt{ADt}} \right).$$

The first case corresponds to a situation in which the oxygen atoms during the technological operations of grinding, the aging of the powder up to the moment of pressing, are adsorbed on the surface in a certain amount of  $N$ , and their diffusion into the sample takes place over a much longer period of time, in particular when the powder is already compressed and new oxygen atoms are not have access. The second case is likely to occur when adsorption and diffusion occur simultaneously until the powder is pressed.

It should also discuss another option. Despite the high density of the sample, it contains about 0.01 bulk portions of the pore [8]. If the volume of sample  $V$  is  $\approx 0.4 \text{ cm}^3$  ( $h = 8 \text{ mm}$ ,  $d = 8 \text{ mm}$ ) and the pore volume is  $1\% \equiv 0.004 \text{ cm}^3$  and if the pore pressure is equal to the compression pressure (2 GPa), the concentration of oxygen atoms in pores is (in the approximation of the ideal gas)  $n \approx 0.5 \cdot 10^{24} \text{ cm}^{-3}$ . If the pressure in pores is equal to atmospheric, then  $n \approx 0.5 \cdot 10^{20} \text{ cm}^{-3}$ . Multiplying this number by the volume of the pore we find the number of oxygen atoms in the sample:  $0.5 \cdot 10^{24} \cdot 0.4 \cdot 10^{-2} = 0.2 \cdot 10^{22}$  at. That is, the concentration of the oxygen atoms in the sample can be  $0.2 \cdot 10^{22} \text{ at.} \cdot 0.4 \text{ cm}^{-3} = 0.8 \cdot 10^{21} \text{ cm}^{-3}$ . This large number of oxygen atoms in the process of diffusion can contribute to the formation of p-regions of the material. However, due to the low number of such pores, it can be assumed that due to diffusion there will be formed some local islets of p-type conductivity, which probably will not even be interconnected. Therefore, the simultaneous adsorption and diffusion at the initial stage of samples preparation is more truthful.

According to [1], the diffusion coefficient of oxygen in PbTe is  $10^{-12} \text{ cm}^2/\text{s}$  at room temperature. The result of the calculation using this value is presented in fig. 3. It can be seen that, in the case of a limited source, and in the case of an unbounded  $\approx 5 \mu\text{m}$  distance, the concentration of oxygen is comparable with the measured Hall's concentration of carriers. For calculation by the formula (1) we took  $A = 10^{15} \text{ cm}^{-2}$ , which corresponds to the monolayer of the oxygen on the grain surface, and by formula (2) –  $N_0 = 10^{18} \text{ cm}^{-3}$ . For both cases, the diffusion time was 10 h, the temperature was  $\approx 300 \text{ }^\circ\text{C}$ .

Thus, even in comparison with relatively large grains, the thickness of the layer in which oxygen can determine the nature of the electrophysical properties is significant. The fact that the properties of this layer are determined only by the impurity can be evidenced by the fact that the carrier concentration is almost constant, at least, to a temperature of  $150 \text{ }^\circ\text{C}$ . In this case, it can be assumed that the central part of the grain will be unoxidized, and its conductivity will be determined by its own carriers.

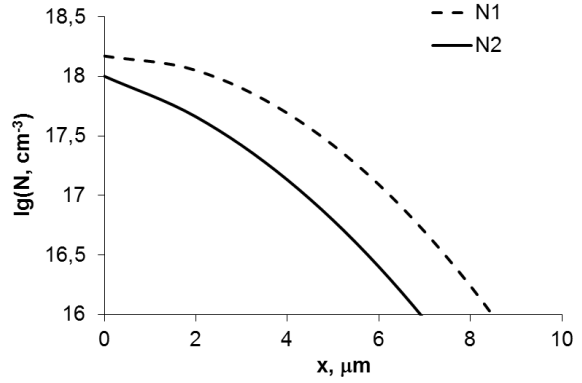


Fig. 3 – Estimated distribution of oxygen atoms on the depth of the sample for two probable mechanisms:  $N_1$  is a limited source ( $A = 10^{15} \text{ cm}^{-2}$ ),  $N_2$  is an unlimited source ( $N_0 = 10^{18} \text{ cm}^{-3}$ ).  $D = 10^{-12} \text{ cm}^2/\text{s}$ ,  $t = 10 \text{ h}$ ,  $T = 300 \text{ }^\circ\text{C}$ .

Representation of the dependence of  $\sigma(T)$  in the coordinates  $\lg(\sigma) \cdot \lg(T)$  gives an opportunity to make conclusions about the conduction mechanisms in the temperature range to the  $p$ - $n$  transition. Assuming that the concentration of carriers has become practically constant up to the  $p$ - $n$  transition temperature, then the temperature dependence of the conductivity will be determined by the temperature dependence of the mobility. And the last one temperature dependence can be represented according to [12] as:

$$u \sim m^*(T)^t T^{-r}.$$

Here  $m^*$  is the effective mass,  $r$  is the carrier dispersion parameter. Considering the fact, that the effective mass of light holes is also a function of temperature ( $m \sim T^{0.5}$ ), then the dependence (3) can be represented as:

$$u \sim T^{0.5t-r*}.$$

It is known [12] that in the absence of degeneracy, the main mechanisms of carrier dispersion are scattering on acoustic phonons ( $0.5t-r = -2.25$ ). For our samples, the degree of temperature dependence  $\sigma(T^\gamma)$ ,  $\gamma \approx -2.5$ , if the sample was not annealed and  $\gamma = -3.0$  for samples that have been annealed at  $500 \text{ }^\circ\text{C}$ . That is, the temperature dependence of the conductivity can be explained on the assumption the decisive influence of acoustic phonons scattering, and minor changes in the inclination of this dependence after annealing can be explained by the presence of some additional mechanism.

It is worth noting here that at the temperature range ( $150$ - $200$ )  $^\circ\text{C}$  the influence of the carriers at heavy holes zone on the kinetic properties will be significant, the distance to this zone decreases with increasing temperature and at  $\approx 200 \text{ }^\circ\text{C}$  becomes zero [9]. It is also possible the influence of own carrier's concentration that growth with temperature. Although this effect will be the same for both non-annealed and annealed samples, the analysis of the dependence of  $\sigma(T)$  is a rather complicated task.

In order to verify the assumptions made above regarding the possible scattering mechanisms, the theo-

retical calculation of the conductivity temperature dependence with taking into account the scattering on acoustic phonons, and the mechanism of the carriers passage through the grains boundaries as a result of electron emission has been spent.

The mobility of carriers under scattering by phonons, according to [13], is defined as:

$$u = e \left\langle \frac{\tau(E)}{m^*(E)} \right\rangle.$$

For a two-zone approximation [13]:

$$\tau(E) = \tau_0(T) \frac{(x + \beta x^2)^{r-\frac{1}{2}}}{(1 + 2\beta x)},$$

$$m^*(E) = m_0^*(1 + 2\beta x).$$

The value of  $\tau_0(T)$  in (5) is determined separately for each of the possible scattering mechanisms which in terms are characterized by the parameter  $r$ . In particular at scattering on acoustic phonons  $r = 0$  [13]:

$$\tau_0(T) = \frac{2\pi\hbar^4 \rho v_0^2}{(2m^* k_0 T)^{\frac{3}{2}} E_1^2},$$

where  $\rho$  is the crystal density (8.24 g/cm<sup>3</sup>),  $v_0$  is sound speed in the crystal (3.6 · 10<sup>5</sup> cm/s),  $E_1$  is the deformation constant (15 eV [14]). Then:

$$u = e \frac{\tau_0(T)}{m^*} \left\langle \frac{(x + \beta x^2)^{r-\frac{1}{2}}}{(1 + 2\beta x)^2} \right\rangle.$$

Average value of parameter  $\langle A \rangle$ , according to [13]:

$$\langle A \rangle = \frac{1}{3\pi^2 n_0} \int_0^\infty \left( -\frac{\partial f}{\partial E} \right) k(E)^3 A(E) dE,$$

where

$$n = \frac{(2m^* kT)^{\frac{3}{2}}}{3\pi^2 \hbar^3} I_{3/2,0}^0(\eta, \beta).$$

Taking the dispersion law for the zone

$$k = \sqrt{\frac{2m^*}{\hbar^2}} E \left( 1 + \frac{E}{E_g} \right), \text{ expression for mobility:}$$

$$u = e \frac{\tau_0(T)}{m^*} \cdot \frac{I_{r+1,2}^0(\eta, \beta)}{I_{3/2,0}^0(\eta, \beta)}.$$

For dual-zone Kain model two-parameter Fermi integrals according the [13]:

$$I_{n,k}^m(\eta, \beta) = \int_0^\infty \left( -\frac{\partial f_0}{\partial x} \right) \frac{x^m (x + \beta x^2)^n dx}{(1 + 2\beta x)^k}.$$

In represented expressions [13]

$$x = \frac{E}{k_0 T}, \quad \eta = \frac{\mu}{k_0 T}, \quad \beta = \frac{k_0 T}{E_g},$$

$$f_0 = \frac{1}{1 + e^{x-\eta}}, \quad -\frac{df_0}{dx} = \frac{e^{x-\eta}}{(1 + e^{x-\eta})^2}.$$

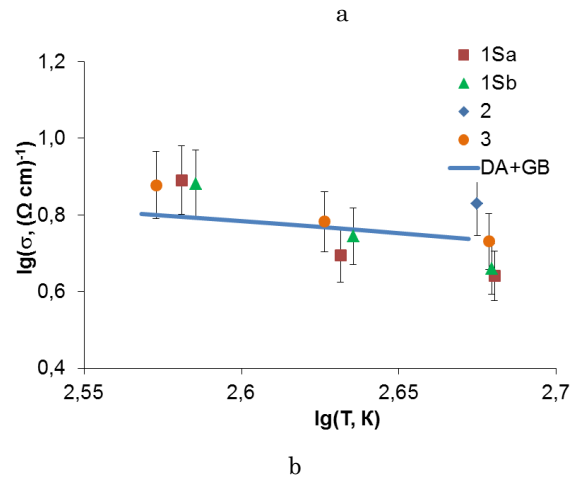
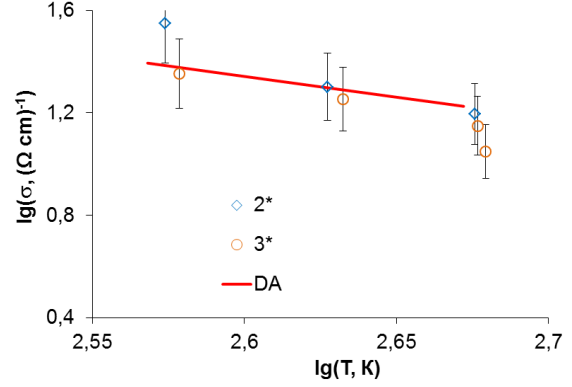


**Fig. 4** – The logarithm dependence between the specific conductivity and the temperature of the annealed (a) and non-annealed (b) samples. The curve on fig. (a) is the calculation based on the model of carriers scattering on acoustic phonons, in fig. (b) considering scattering by acoustic phonons and electronic emission.

Assuming that in the studied range of temperatures, the role of light holes is decisive, the calculated mobility values are several hundred cm<sup>2</sup>/(V·s), and the conductivity calculated with their use significantly exceeds the experimental values. If we assume that the role of heavy holes is decisive, then the calculated curve  $\sigma(T)$  practically coincides with the experimental dependence for the annealed samples on the interval before the p-n transition. It is important to note that we did not use any additional variation parameters at the calculations. A slight discrepancy between the temperature coefficient of this dependence can be explained by some influence of light holes and effect of the other possible scattering mechanisms.

In the case of thermoelectronic emission, the carrier mobility is determined according to the expression [15]:

$$u = L e_0 \left( \frac{1}{2\pi m^* kT} \right)^{1/2} \exp\left(-\frac{E_b}{kT}\right).$$

Here  $L$  is the grain size,  $E_b$  is the energy of the barrier.

Considering the above two mechanisms, and varying the value of  $E_b$ , at a value of 10 meV, a satisfactory correlation with the experimental data was achieved. It should be noted that in [14], for samples of PbTe, the result obtained by pressing the nanodispersed lead telluride powder is 60 meV, which, in magnitude, correlates with our determined value.

Also, with these data it is possible to estimate the surface concentration of oxygen atoms, using the dependence [14]  $E_b = \frac{q^2 A^2}{8\epsilon\epsilon_0 n_H}$ . The resulting value

$A \approx 10^{16}$  at/cm<sup>2</sup> correlates with the one used for calculation of the oxygen diffusion profile value.

### Ефекти взаємодії кисню з поверхнею РbTe та їх вплив на термоелектричні властивості матеріалу

I.V. Gorichok<sup>1</sup>, V.V. Prokopyv<sup>1</sup>, P.I. Zaphulyak<sup>1</sup>, O.M. Matkivskiy<sup>1</sup>,  
T.O. Semko<sup>1</sup>, I.O. Savelikhina<sup>2</sup>, T.O. Parashuk<sup>3,\*</sup>

<sup>1</sup> Прикарпатський національний університет імені Василя Стефаника, вул. Шевченка, 57, 76018, Івано-Франківськ, Україна

<sup>2</sup> Івано-Франківський національний медичний університет, вул. Галицька 2, 76018, Івано-Франківськ, Україна

<sup>3</sup> Інститут виробництва передових технологій, вул. Вроцлавська, 37, 30-011, Краків, Польща

Представлено результати дослідження термоелектричних властивостей отриманих методом пресування порошку зразків телуриду свинцю. Показано, що адекватна модель структури пресованих зразків повинна враховувати наявність приповерхневого шару, утворення якого пов'язане із взаємодією матеріалу з атмосферним киснем. Проведено розрахунок рухливостей носіїв у зразках з врахуванням механізмів розсіювання носіїв на акустичних фонах та термоелектронної емісії.

**Ключові слова:** Плюмбум Телурид, Термоелектричні Параметри, Дифузія, Окиснення Поверхні.

### СПИСОК ЛІТЕРАТУРЫ

1. E.H.C. Parker, D. Williams, *Thin Solid Films* **35**, 373 (1976).
2. M. Green, M.J. Lee, *J. Phys. Chem. Solids*, **27**, 797 (1966).
3. L.S. Palatnik, L.G. Petrenko, Yu.A. Volkov. *Sol. St. Phys.* **15** No 5, 1427 (1973).
4. I.V. Kalytchuk, *PCSS* **4** No 3, 505 (2003) [In Ukrainian].
5. E.I. Rogacheva, I.M. Kryvulkin. *Sol. St. Phys.* **43** No 6, 1000 (2001).
6. D.M. Freik, B.S. Dzundza, M.A. Lopyanko, Ya.S. Yavorsky, A.I. Tkachuk, R.B. Letsyn, *J. Nano- Electron. Phys.* **4** No 2, 02012 (2012).
7. R.Ya. Popylsky, Yu.E. Pivinsky, *Pressing of powder ceramic masses 176* (Moscow: Metallurgy, 1983) [in Russian].
8. I.V. Horichok, I.M. Lishchynskij, S.I. Mudryj, O.S. Oberemko, T.O. Semko, I.M. Hatsevich, O.M. Matkivsky, G.D. Mateik, R.O. Dzumedzey, *SEMST* **14** No 3, 53 (2017).
9. D.M. Freik, I.V. Horichok, M.V. Shevchuk, L.V. Turovska, *PCSS* **12** No 2, 378 (2011) [in Ukrainian].
10. D.M. Freyk, I.V. Horichok, Y.V. Lysyuk, L.Y. Mezhylovska, *SEMST* **2** No 8, 37 (2011).
11. Ya.P. Salij, *PCSS* **9** No 2, 235 (2008) [in Ukrainian].
12. S.B. Atakulov, S.M. Zaynolobidinova, G.A. Nabiev, M.B. Nabyev, A.A. Yuldashev, *PTS*, **47** No 7, 869 (2013).
13. B.M. Askerov, *Electronic phenomena of transfer in semiconductors*, 320 (Moscow: Science, 1985).
14. J. Martin, Li Wang, Lidong Chen, G.S. Nolas, *Phys. Rev. B*, **79**, 115311 (2009).